Journal of Catalysis 269 (2010) 44–52

Contents lists available at ScienceDirect

Journal of Catalysis

journal homepage: www.elsevier.com/locate/jcat

Influence of Al_2O_3 on the performance of CeO_2 used as catalyst in the direct carboxylation of methanol to dimethylcarbonate and the elucidation of the reaction mechanism

Michele Aresta [a,*], Angela Dibenedetto [a], Carlo Pastore [a], Antonella Angelini [a], Brunella Aresta [b], Imre Pápai [c]

[a] Department of Chemistry and CIRCC, University of Bari, Campus Universitario, 70126 Bari, Italy
[b] Istituto di Cristallografia, CNR, via Amendola 122, 70126 Bari, Italy
[c] Chemical Research Centre – HAS, Institute of Structural Chemistry, 1525 Budapest, P.O. Box 17, Hungary

ARTICLE INFO

Article history:
Received 10 July 2009
Revised 5 October 2009
Accepted 19 October 2009
Available online 20 November 2009

Keywords:
Methanol carboxylation
Dimethyl carbonate
Effect of Al_2O_3 on CeO_2 catalysts
Surface modification
Surface techniques
DRIFT studies
NMR solid state and solution
Reaction mechanism

ABSTRACT

In this paper we show that modification of ceria by loading alumina strongly reduces the oxidation of methanol and the consequent reduction of Ce(IV) to Ce(III) with increase of both the life of the catalysts and their selectivity. The combination of surface techniques (XPS and BET) with structural techniques (XRD) has allowed a good characterisation of the working catalysts. Spectroscopic analyses (DRIFT and multinuclear solid state and solution NMR) have permitted the monitoring of the species formed on the surface of the catalyst and released from it. The formation of DMC takes place in successive steps such as (i) interaction of methanol with the catalyst surface with the formation of the surface-bound —OCH_3; (ii) building on the catalyst surface of the hemicarbonate moiety [–OCH_3 → –$OC(O)OCH_3$]; and (iii) reaction of the latter with the gas-phase methanol to afford the organic carbonate.

1. Introduction

The direct carboxylation of alcohols to dialkylcarbonates (and in particular of methanol to dimethylcarbonate – DMC, the most popular of such class of compounds) is attracting much attention worldwide because of its potential industrial application. Considering DMC, it is used as a monomer for polymers [1,2], for the production of other carbonates (such as diphenylcarbonate) via trans-esterification [3–7], as alkylating or carboxylating agent [8–14], in the agrochemical [15] and pharmaceutical industry [16–19]. A new potential application of some dialkylcarbonates is as additives to gasoline that would greatly expand their market. New synthetic methodologies are required because those on stream, either the one based on the use of phosgene (Eq. (1)) or the most recent one based on the oxidative carbonylation of methanol (Eq. (2)) [20–23], suffer from several drawbacks that prevent the expansion of the production to the desired scale.

$$2ROH + COCl_2 + 2NaOH \rightarrow (RO)_2CO + 2NaCl + 2H_2O \quad (1)$$

$$2CH_3OH + 1/2O_2 + CO \xrightarrow{CuCl_2} (CH_3O)_2CO + H_2O \quad (2a)$$

$$2CH_3OH + 1/2O_2 + CO \xrightarrow{Pd/NO} (CH_3O)_2CO + H_2O \quad (2b)$$

The direct carboxylation of alcohols (Eq. (3)), a reaction that responds to the principles of the sustainable chemical industry, is being investigated worldwide by several research groups.

$$2ROH + CO_2 \rightarrow (RO)_2CO + H_2O \quad (3)$$

Both homogeneous and heterogeneous catalysts have been used so far. Among the former, Sn [24,25] and Nb [26,27] show interesting properties. Nevertheless, their exploitation is limited by the conversion of tin catalysts into oligomers during catalysis that reduces their activity; while Nb(V)-alkoxo species maintain their activity until they are in an almost anhydrous reaction medium. Unfortunately, water formed in reaction (3) may cause the de-activation of the catalyst. In order to prevent such negative situation, energy-consuming methodologies have been implemented, such as the recovery of the catalyst at the end of each reaction cycle and its re-use in anhydrous alcohol and the dewatering of the reaction solution using water traps. Organic water traps such as aldols [28], ketals [29] and ortoformates [30], although rise the problem of their separation from the reaction mixture and conversion into the original products, are more efficient than inorganic systems

* Corresponding author. Fax: +39 080 544 36 06.
E-mail address: m.aresta@chimica.uniba.it (M. Aresta).

0021-9517/$ - see front matter © 2009 Elsevier Inc. All rights reserved.
doi:10.1016/j.jcat.2009.10.014

such as zeolites as the latter at the temperature used in catalysis (around 420 K) may act as protonating agents of DMC, reversing the reaction. Using zeolites, cooling of the reaction mixture to room temperature or lower, dewatering and reheating have been [31] also used that implies a large use of energy considering the energy needed for water elimination from the zeolites if they have to be recycled. Dicyclohexylcarbodiimide, DCC [32], alone is able to promote the formation of dialkylcarbonates under mild conditions (330 K and 0.2 MPa) with excellent yield (>90%) and selectivity (>98%), but one mol of DCC is converted into the relevant urea-DCU (Eq. (4)) per mol of DMC produced. The recently achieved back-conversion of DCU into DCC [32b] may make useful such synthetic methodology that may find a practical interest in the synthesis of niche-carbonates.

$$\underset{\text{DCC}}{\text{CyN=C=NCy}} + 2\,CH_3OH + CO_2 \rightarrow DMC + \underset{\text{DCU}}{\text{CyHNC(O)NHCy}} \qquad (4)$$

Heterogeneous catalysts appeared to be more promising. CeO_2 [33,34], ZrO_2 [35,36] and TiO_2 [37] have been used but they in general suffer from a serious drawback represented by their de-activation: after the first cycle, their activity decreases to a marginal conversion of methanol. In order to understand the reasons of such de-activation and to discover a remedy for preparing long-living catalysts, we have started an investigation project aimed at proving the reaction mechanism of the carboxylation and discovering the key parameters that may help in designing new resistant catalysts. In this paper, we describe the results of our spectroscopic and structural studies on ceria and Al_2O_3-loaded-ceria used as catalysts in the carboxylation of methanol and the evidences which support the reaction mechanism.

2. Materials and methods

All solvents, starting reagents and the commercial metal oxides were RP Aldrich products. Alcohols were dried, distilled [38] and stored under dinitrogen (the residual water was 20 ppm, as determined by the Karl-Fisher method, using a Metrohm 785 DMP Titrino apparatus). Carbon dioxide was from Rivoira IP (99.999% purity).

Multinuclear Nuclear Magnetic Resonance-NMR solution experiments were carried out with a Bruker AVANCE apparatus operating at 600 and 242.9 MHz for ^1H and ^{13}C, respectively. The ^{13}C CP-MAS NMR experiments were acquired on a 400 MHz Varian INOVA apparatus (9.39 T) operating at 100.1 MHz for ^{13}C and at 104.215 MHz for the ^{27}Al nucleus. The solid samples were packed in a 5 mm *od* zirconia rotor and spined at 7 kHz during the analysis. The 90° pulse duration was 4.5 μs with a subsequent relaxation time of 4 s. The number of transients changed with the aluminium content in order to obtain good spectra in terms of signal-to-noise ratio. All the chemical shifts were calculated taking as reference an aqueous solution of aluminium as $[Al(H_2O)_6]^{3+}$.

FTIR-DRIFT spectra were recorded with a Shimadzu Prestige 21 instrument equipped with the Shimadzu DRS-8000 basic apparatus modified for our purposes.

X-ray Photoelectron Spectroscopy – XPS spectra were obtained using a ThermoVG Thetaprobe spectrometer, equipped with a microspot monochromatised Al Kα source and the gun of low-energy electrons for compensation of electrostatic charging of samples. The Al Kα line (1486.6 eV) was used throughout this work and the base pressure of the instrument was 10^{-9} mbar. Survey scans (binding energy range 0–1200 eV, FAT mode, pass energy = 200 eV) and detailed spectra (FAT mode, pass energy = 50 eV) were recorded for each sample. Data analysis of the latter was performed using the Avantage software package, which consists of a non-linear least squares fitting program. The values of binding energies BE (eV) were taken relatively to the binding energy of Cls-electrons of hydrogencarbonate-HCO_3^- on the sample surface (produced by adventitious carbon), which is accepted to be equal to 285.0 eV. Quantification was performed using peak areas; comparison between data from different elements was possible after correction (division) by empirically derived atomic sensitivity factors.

X-ray diffraction patterns-XRD patterns were taken using a Bruker D8-DISCOVER diffractometer in reflection geometry using a flat sample, with a X-ray tube using the Cu Kα1 line (λ Kα1 = 1.54056 Å and λ Kα2 = 1.54439 Å). The tests were done in a short period of time so that the same experimental conditions were preserved. The experimental parameters were step-scan 0.03°, 2θ range from 25° to 135°, 20 s acquisition time.

XRD-patterns were compared with different diffraction patterns of cerium oxide present in PDF (Powder Diffraction File) data bank using DIFFRACplus EVA [39] for qualitative analysis to check out the chemical phase present in the powder. XRD-patterns data were processed using EXPO2006 [40] for structural analysis and FullProf/Topas [41,42] for structural refinement according to the Rietveld method [43]. The peak profiles were fitted with Pearson VII function to calculate the crystallite size and the full-width at half-maximum (FWHM).

BET areas were determined with a Micromeritics Chemisorb 2750 equipment.

GC–MS analyses were carried out with a gas chromatograph Shimadzu 17 A (capillary column: 30 m; MDN-5S; ∅ 0.25 mm, 0.25 μm film) coupled to a Shimadzu QP5050 A mass spectrometer. Quantitative determinations on the reaction solutions were performed using a Hewlett Packard 6850 GC-FID (capillary column: 30 m; Carbowax; ∅ 0.25 mm, 0.25 μm film).

2.1. Synthesis of 3% and 10% Al/Ce-mixed oxides

These catalysts were prepared following the procedure described in [44a]. The solid was then calcinated in the air at 823 or 923 K for 3 h to obtain the Al/Ce-mixed oxides. XPS and XRD analyses were used to characterise the oxide as reported in Section 3. The BET area was 74.5 ± 1.3 and 43.2 ± 1.5 m^2/g^{-1} for the 3% Al_2O_3 sample calcinated at 823 and 923 K, respectively. The BET area of the 10% Al_2O_3-loaded ceria was 88.5 ± 1.7 and 57.0 ± 1.7 m^2/g^{-1} for the sample dried at 823 and 923 K, respectively. Each value was the average of three independent measurements.

The ^{27}Al CP-MAS NMR spectrum of the CeO_2 samples loaded with Al at 3% and 10% shows that both samples exhibit a net signal at 40 ppm (attributed to "dispersed" alumina in the literature [44a,45]) not found in Al_2O_3. The intensity of such signal grows with the content of Al_2O_3 and it is higher in the sample with 10% than in the sample with 3% loaded Al_2O_3. A further increase of the content of Al_2O_3 causes the appearance of the signals of free Al_2O_3 besides the signal at 40 ppm. In particular a signal at 55 ppm that can be attributed to a tetra-co-ordinated tetrahedral Al and a signal at 7.4 ppm that can be attributed to a six-co-ordinated octahedral Al peak out.

2.2. Catalytic tests

The reaction of carboxylation of alcohols was run at 5.0 MPa, 408 K for a time from one to three hours in the batch 4×-parallel reactor (in mono- or bi-phasic conditions, Fig. 1) that allows the withdrawal of the reaction gas or liquid for analysis during the reaction.

Typically, 50 mg of catalyst, 4 mL of dry methanol and a pressure of 5.0 MPa of CO_2 were charged in each well of the 4×-parallel reactor (the volume of each well was 20 mL), then the temperature was increased to 408 K. The measured thermodynamic conversion

Fig. 1. 4×-parallel stainless steel autoclave with continuous sampling of gas and liquid.

of the alcohol into DMC was 0.45–0.7% in 3 h (non-equilibrium conditions, the equilibrium concentration was 2.1% reached after *ca.* 5–8 h). The catalyst was then recovered, dried under vacuum at room temperature, characterised using DRIFT, BET, XPS and XRD, and reused with new fresh dry alcohol.

2.3. DRIFT studies on CeO_2 and on Al_2O_3-loaded-CeO_2 after the catalysts exposure to CH_3OH and CH_3OH–CO_2

The DRIFT cell was purged with a dry dinitrogen flow to avoid water contamination of the sample when the pure oxides were monitored. The reaction with methanol was carried out in a flow reactor as discussed below. For studying the reaction with CO_2 either the catalyst bearing the $-OCH_3$ moiety bound on the surface was loaded in the DRIFT cell which was then flushed with a flow of dry CO_2, or the catalyst was treated in the 4×-parallel reactor (Fig. 1) in which it was possible to run four parallel tests at the same temperature. As an example, CeO_2 plus methanol, CeO_2 plus methanol–CO_2 at 0.1 MPa, 10% Al_2O_3/CeO_2 plus methanol and 10% Al_2O_3/CeO_2 plus methanol–CO_2 were charged into the four wells of the reactor and the reaction was performed for the established time; the gas phases were then withdrawn and singularly analysed while the solid catalysts were analysed by DRIFT. The results are discussed in Section 3.

2.4. Study of the reaction mechanism by using multinuclear solid state and solution NMR

The sample of the CeO_2/Al_2O_3-calcinated catalyst (0.5 g) was reacted with gaseous methanol at 408 K using the flow reactor depicted in Fig. 2. The catalyst was recovered and dried at room temperature until excess methanol was eliminated. The catalyst was then analysed by solid state ^1H and ^{13}C NMR. The sample was treated with CO_2 at 408 K and re-analysed as mentioned above.

The carboxylated catalyst was then divided into four portions. One was directly heated at 408 K in the absence of methanol in the solid state, and the gas phase and the solid were analysed using GC–MS and solid state NMR, respectively. The second was suspended in toluene and heated at the same temperature in the autoclave: the liquid phase was then analysed by GC–MS and NMR. The third portion was treated with gaseous methanol at 408 K in a flow reactor (Fig. 2) and then the catalyst and the liquid phase were analysed by solid state or solution ^1H and ^{13}C NMR, respectively. The fourth portion was heated in toluene-containing methanol at 408 K; the solution was analysed by ^1H and ^{13}C NMR. The analytical features are presented in Section 3.

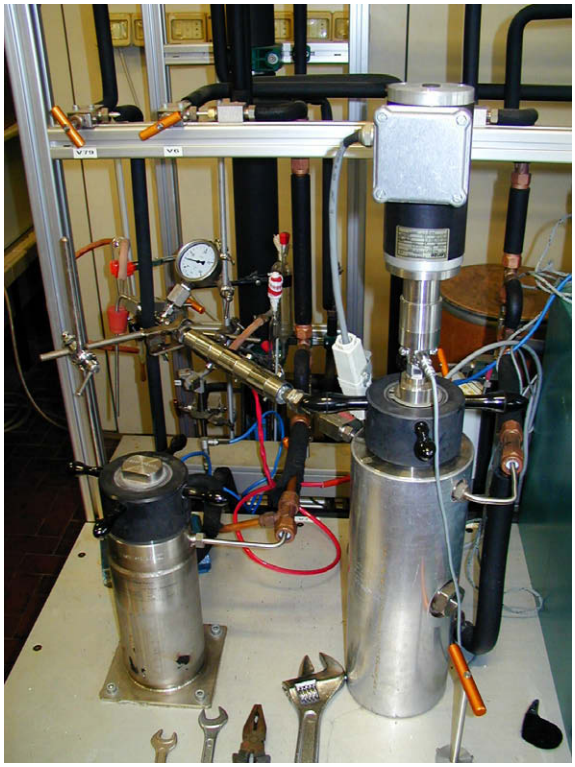

Fig. 2. Flow reactor fed with a sc-single-phase mixture of methanol in CO_2 (molar ratio 1:1, 30.0 MPa, 408 K).

2.5. Computational details

DFT calculations were carried out in order to obtain information on the structures and the reaction pathway energy minima and transition states of the investigated reactions. All calculations were performed at the B3LYP/SDDP level of density functional theory, where B3LYP is the applied exchange-correlation functional [46–48] and SDDP refers to a basis set that includes the Stuttgart–Dresden relativistic small core ECP basis set for niobium and the Dunning/Huzinaga DZ + polarisation all-electron basis set for the lighter atoms [49–52]. The nature of the stationary points obtained from the geometry optimisation was always verified by subsequent vibrational frequency analysis. The solvent effects were included into calculations using the ε coefficient. The calculations were performed using the Gaussian 03 program package [53].

3. Results and discussion

3.1. Characterisation of CeO_2 contacted with only methanol

Commercial CeO_2 (with particle size *ca.* 5 μm) used in the carboxylation of anhydrous methanol at 408 K under 5 MPa of CO_2 [44a,b] deactivates after a few cycles due to several causes, including the reduction of Ce(IV) to Ce(III) that causes the oxidation of methanol [44a]. Fig. 3 shows a typical trend of the variation of DMC yield as the number of runs is increased.

As we have already shown [44], BET and XPS studies confirm that during catalysis the catalyst undergoes a reduction of the surface area (from 8.8 m^2/g to 1.6 m^2/g in this work, see Table 1), while Ce(IV) is partially reduced to Ce(III). The application of the Shyu method [54] has allowed to calculate a 20 ± 2% reduction of Ce(IV) to Ce(III). CeO_2 synthesised (particle size 5–20 nm) in this work shows a much higher stability (see Fig. 3).

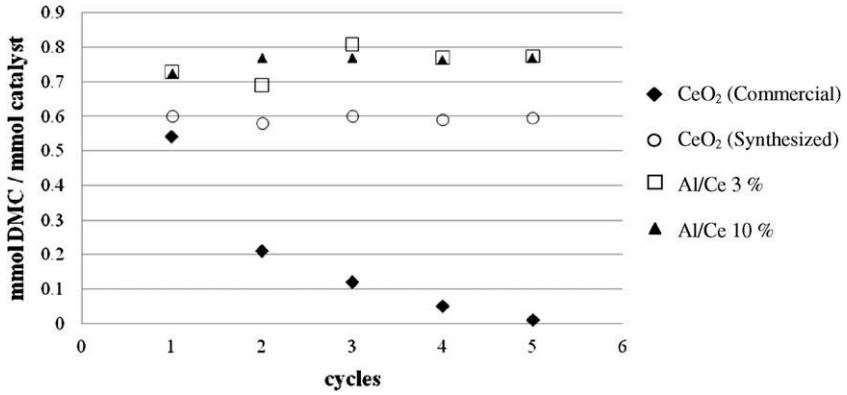

Fig. 3. DMC yield in five consecutive cycles of reaction. In each cycle the same amount (50 mg) of CeO_2 was placed in a reactor with 4 mL of methanol, at 408 K for 3 h under 5.0 MPa of carbon dioxide.

Table 1
BET surface area of several catalysts.

Entry	Oxide	BET surface (m^2/g)
1	CeO_2 commercial	8.8 ± 1.1
2	CeO_2 commercial after use[a]	1.6 ± 0.6
3	CeO_2 synthesised, calcinated at 923 K	25.1 ± 1.1
4	CeO_2 synthesised, calcinated at 923 K after use[a]	19.8 ± 1.3
5	3%Al/Ce calcinated at 823 K	74.5 ± 1.4
5	3%Al/Ce calcinated at 823 K after use[a]	69.5 ± 1.3
6	3%Al/Ce calcinated at 923 K	43.2 ± 1.5
7	3%Al/Ce calcinated at 923 K after use[a]	40.7 ± 1.4
8	10%Al/Ce calcinated at 823 K	88.5 ± 1.7
9	10%Al/Ce calcinated at 923 K	57.0 ± 1.7
10	10%Al/Ce calcinated at 923 K after use[a]	55.0 ± 1.2

[a] The surface has been measured after three cycles in catalysis.

XRD profiles confirm that after use in catalysis the bulky cell structure of the commercial ceria remains essentially that of the starting material [44a], but an increase of crystallinity is observed as demonstrated by the comparison of the full-width at half-maximum (FWHM).

We have now carried out a DRIFT study on the catalyst in order to collect information on the reactions occurring on its surface under the operative conditions and have characterised the species formed and elucidated the reaction mechanism.

Fig. 4 shows the DRIFT spectrum in the range 2000–900 cm^{-1} of micro-particles of commercial CeO_2 at zero time (Fig. 4a) and after 1 h contact with methanol in the absence of CO_2 at 408 K (Fig. 4b), the temperature at which catalysis is run.

The spectrum of commercial CeO_2 does not show any signal in the above-mentioned region (Fig. 4a). Conversely, after treatment with methanol it presents new strong bands at 1584, 1574, 1371, 1355, 1097 and 1035 cm^{-1} (Fig. 4b) with respect to that of pure CeO_2. The two latter bands can be ascribed to the methoxo groups $Ce–OCH_3$ formed on the surface of the particles upon interaction with methanol [55–57]. Instead, the bands at 1585 (s), 1574 (sh) and 1355 (s) cm^{-1} are due to the products of oxidation of methanol. They have been assigned to formate-moieties bonded in a chelate mode to two Ce(III)-atoms. For comparison, we recall that chelate formates in several titanium-molecular compounds present a difference between the asymmetric and symmetric vibrations close to 200 cm^{-1} [58]. In terminal formates, instead, the asymmetric stretching is found at higher values than 1630 cm^{-1}, while the symmetric vibrations are generally at lower value than 1350 cm^{-1}, with a difference of $\Delta\nu = \nu_{as} - \nu_s > 280$ cm^{-1} [58]. Our data match those of other DRIFT studies that show that CeO_2 oxidises pure methanol with the formation of several organic products among which formates for which IR bands at 1585 (s), 1563 (sh) and 1358 (s) cm^{-1} have been attributed to *asym-sym* vibrations, respectively [55].

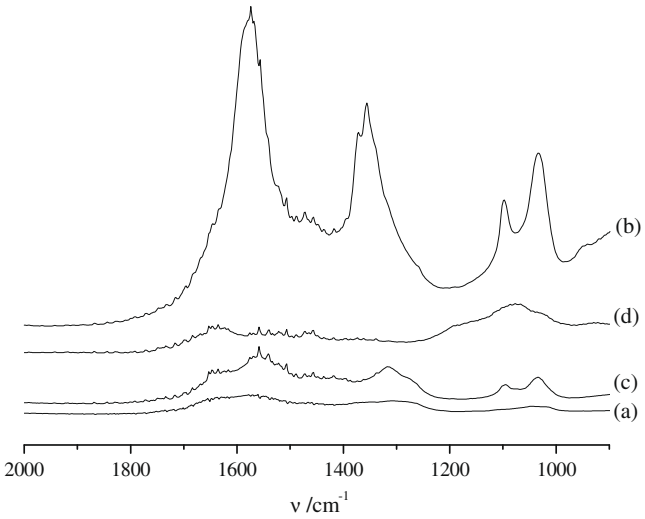

Fig. 4. DRIFT spectrum of (a) commercial CeO_2, (b) commercial CeO_2 after exposure to methanol for 1 h at 408 K, (c) synthesised CeO_2 after exposure to a sc-single-phase CO_2–methanol mixture (1:1 molar ratio) for 1 h at 408 K, (d) CeO_2 loaded with Al after exposition to methanol for one h at 408 K.

Both XPS and DRIFT analyses confirm, thus, that upon contact of CeO_2 with methanol, in the same temperature conditions as during the catalytic carboxylation cycles, the surface of the catalyst may be involved in a red-ox process with Ce(IV) reduction to Ce(III) and concomitant oxidation of methanol. The observation of the XPS spectrum of the O-atom of the catalyst before and after catalysis clearly shows a considerable modification of the O-portion of the spectrum with the rise of the band at 531.5 eV due to Ce(III)–O species that is absent or very weak in the starting material. These features repeat our previous observations [44].

All such surface modifications are correlated to the reduced catalytic activity of ceria [44a]. The catalyst modification progresses with the number of cycles as shown by XPS spectra. On the other hand, the cell parameters do not show any sensible change during the operations: in fact, in both spectra the peak positions for the equivalent Bragg angles are practically the same. The only evident difference, i.e. the broadening of the peaks at large values (>100) of 2θ, may be due to a minor distortion of the structure, which, noteworthy, is not restored with the heating as already noted by other authors [33].

The mode of preparation of the sample of ceria influences its stability. In fact, CeO_2 nanoparticles (around 5–20 nm) synthesised

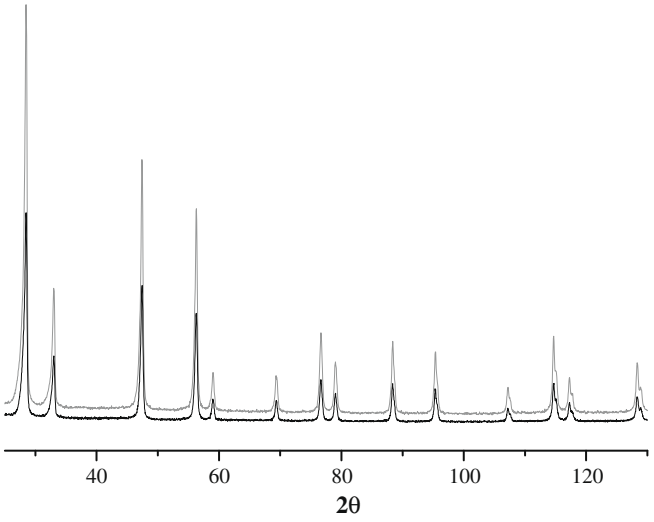

Fig. 5. XRD of commercial (grey line) and synthesised (black line) CeO_2. The latter shows a lower crystallinity as a consequence of its nanoscale dimension with respect to the microscale of the former.

in our laboratory [44] show a much better performance (Fig. 3) with a lower aggregation tendency, a more constant BET and resistance to use. The XRD analysis of the synthesised ceria is shown in Fig. 5 (continuous black line) and compared with the spectrum of commercial ceria (grey line).

The FWHM is larger for the synthesised material than for the commercial material, showing a lower crystallinity justified by the smaller size of the particles which range around 5–20 nm with respect to 5 μm of the commercial sample. The DRIFT spectrum of the synthesised nanocatalyst in the 2000–900 cm^{-1} region is not informative as it is super imposable with that of commercial ceria shown in Fig. 4a.

3.2. DRIFT characterisation of synthesised CeO_2 contacted with methanol or a single-phase sc-CO_2–methanol mixture

When synthesised CeO_2 was contacted with methanol at 408 K in the same conditions as for the commercial sample, the DRIFT spectrum showed bands at 1098 and 1035 cm^{-1} due to the —OCH_3 moiety bonded to the surface. Only very weak signals due to the formate were evident. After contact with a single-phase sc-CO_2–methanol mixture at 408 K (Fig. 4c) the IR spectrum showed new bands at 1572, 1469, 1360 and 1109 cm^{-1} attributed to the hemicarbonate moiety, —$OC(O)OCH_3$ [34,51]. The intensity of the latter signals never grows very much with time if both methanol and CO_2 are present. Conversely, the signals of formate are absent during the whole time of catalysis. These features seem to suggest that the presence of CO_2 somehow prevents the oxidation of methanol. This would be possible if the carboxylation of the surface-bound methoxo moiety was faster than its oxidation. It is worthy to recall that the kinetic constant of CO_2 insertion into a metal-alkoxo bond has been found to range around 10^2–10^4 s^{-1} for homogeneous metal systems [26,27,60,61], and might be of the same order of magnitude for heterogeneous systems. Once the carboxylation of the methoxo moiety occurs, the oxidation to formate or other C1 species is prevented and the reduction of surface Ce(IV) occurs at a much lower extent, if not at all.

3.3. Catalyst modification: CeO_2 loaded with Al_2O_3. Behaviour of the modified catalyst towards methanol and CO_2–methanol

We have reported [44] that CeO_2 loaded with Al_2O_3 presents a longer life than CeO_2 alone, as also shown in Fig. 3. Such behaviour has been encountered in other modified catalysts [62]. Fig. 4d shows the behaviour of the bi-metallic CeO_2–Al_2O_3 catalysts when exposed to methanol at 408 K for 1 h: the bands of the oxidised form of methanol are completely absent. Such features well match the behaviour of the Al/Ce catalysts (loading of 3–10% of Al_2O_3) which have a much better resistance than pure ceria, and does not show any appreciable reduction of Ce(IV) to Ce(III) during catalysis [44] with a selectivity of methanol conversion into dimethylcarbonate practically equal to 100% (no methanol oxidation species were detected in the reaction mixture).

The XRD and XPS spectra show that the cell structure and the surface properties of the Al/Ce catalyst are identical with those of the starting material [44] indicating that there is no Ce substitution with Al, that is quite obvious because of the large difference of the atomic radii of Ce (1.04 Å) and Al (0.5 Å) [61,63].

Therefore, the CeO_2 surface modification produced by Al has the double effect of reducing the oxidation of methanol and improving the carboxylation of the methoxo group.

3.4. The BET properties of the Al-loaded ceria catalysts

An important feature of the loading of Al_2O_3 on CeO_2 is the increase of the surface area. As Table 1 shows, the surface area can be increased by almost one order of magnitude by loading Al_2O_3 (compare Entries 1 and 5). The area is also dependent on the temperature at which the catalyst is calcinated (compare Entries 5,6 and 8,9 in Table 1).

The other significant distinctive feature of the Al_2O_3-loaded ceria with respect to pure ceria is the very minor variation of the BET area before and after use in catalysis. Entries 3 and 4 in Table 1 show that the area is reduced by 20% with pure synthesised ceria, while it decreases by only a few points per cent (from 1.3 to a maximum of 7%) with Al-loaded ceria. The loading of Al_2O_3 on CeO_2 confers, thus, to the catalysts a longer life coupled to an excellent selectivity.

3.5. The study of the reaction mechanism

Schemes 1–3 present the putative steps which occur in the formation of DMC from methanol and CO_2. Steps *a*–*b* in Scheme 1 or *a*′–*b*′ in Scheme 2 are likely routes [59,64] to the formation of the anchored –OCH_3 moiety which reacts with CO_2 to afford the hemicarbonate –$OC(O)OCH_3$ moiety. It has been proposed [59,64] that step (*d*) in Scheme 2 may generate DMC. Noteworthy, such mechanism reminds what has been found with "$^{n}Bu_2Sn(OMe)(OCOOMe)$" [24,25] that is able to produce DMC *via* and intramolecular methyl transfer from the –OCH_3 to the –$OCOOCH_3$ moiety when heated in toluene. Such methyl transfer on the heterogeneous catalyst surface may have a lower probability than that in the homogeneous species which have much better defined structural features. In the heterogeneous catalyst, in fact, the probability that an hemicarbonate moiety and a methoxo-group are placed within an interaction distance in order so that the methyl transfer may occur, is much lower than that in the homogeneous catalyst. An alternative to the methyl transfer from a surface-bound methoxo to a surface-bound hemicarbonate is the gas-phase methanol attack on the surface-bound hemicarbonate moiety.

It is also worthy to note that if an hemicarbonate moiety is within an interaction distance with surface-bound OH groups, that is likely to occur, methylcarbonic acid could be released [65] that quickly converts (Scheme 1, step *c*) into gaseous methanol and CO_2 under the reaction conditions. When the reaction of the hemicarbonate with gas-phase methanol is considered, it may have a high probability to occur while considering the abundance of methanol in the gas mixture that may generate a high concentration around the hemicarbonate moiety bound to the surface,

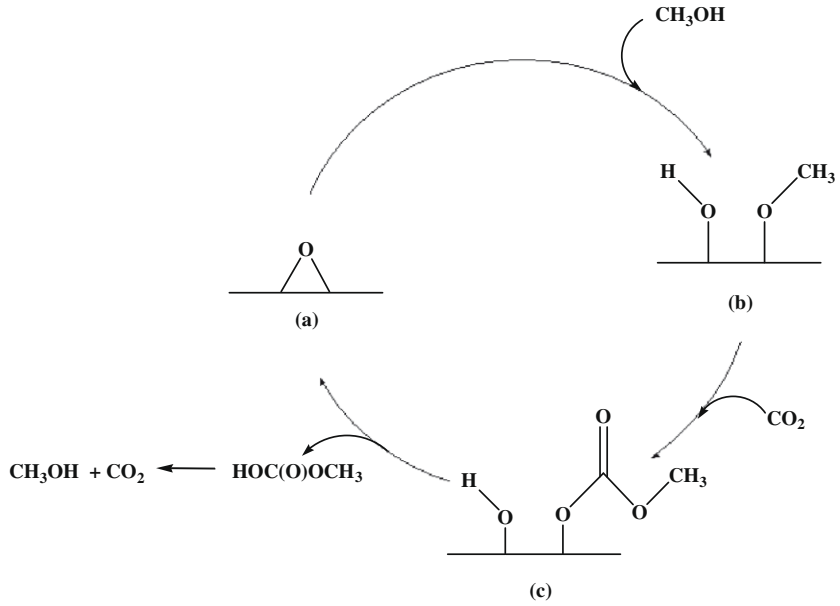

Scheme 1. Putative steps for the formation of methylcarbonic acid from methanol and CO_2.

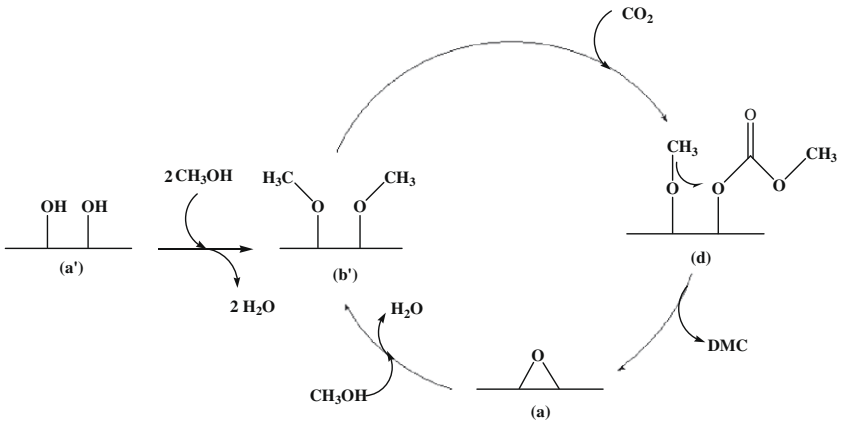

Scheme 2. Putative steps for the formation of DMC from methanol and CO_2 *via* methyl transfer from surface-bound OCH_3 to surface-bound $OCOOCH_3$.

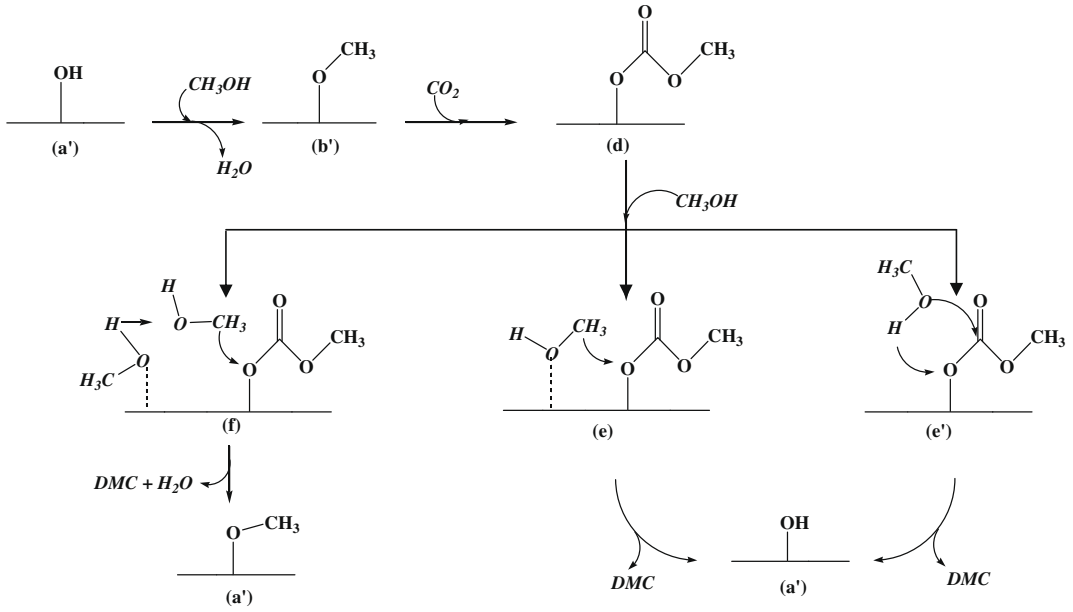

Scheme 3. Putative steps for the formation of DMC from methanol and CO_2 *via* gas-phase methanol attack onto surface-bound $OCOOCH_3$. Gas-phase species are in italics.

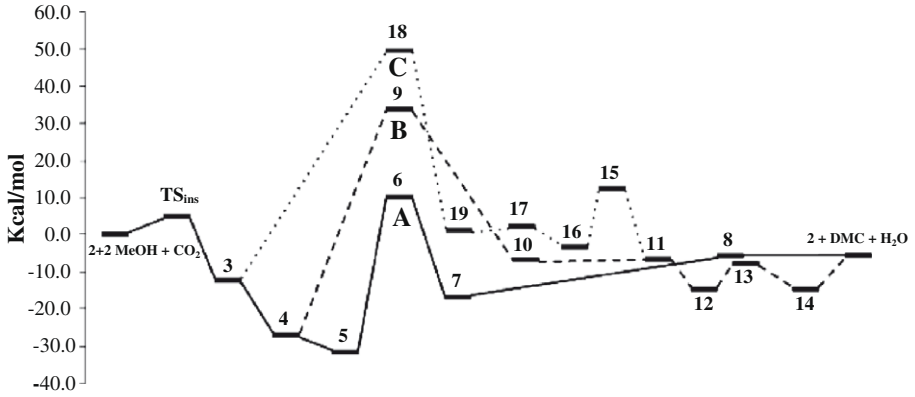

Scheme 4. Comparison of three possible mechanisms for the formation of DMC. Route A: intermolecular attack by two methanol molecules to the hemicarbonate moiety bound to Nb. Route B: intermolecular attack by a single methanol moiety onto the hemicarbonate moiety bound to Nb. Route C: intramolecular methyl transfer from $-OCH_3$ to $-OC(O)OCH_3$.

either one molecule of methanol (Scheme 3, step *e* or *e*′) or two molecules (Scheme 3, step *f*) may be involved in the formation of DMC. We have comparatively studied through DFT such alternative reaction paths using $Nb(OMe)_4(OCOOMe)$ as a probe molecule and an example of a "single site reaction" on the surface of the heterogeneous catalyst. Scheme 4 shows the relative energy profile of three different mechanisms of formation of DMC promoted by $Nb(OCH_3)_4(OCOOCH_3)$, that may find a counterpart in the catalysis occurring on heterogeneous catalysts, namely, (a) the intermolecular attack of two molecules of methanol on the hemicarbonate (compare to step *f* in Scheme 3); (b) the intermolecular attack by one methanol on the hemicarbonate (compare to step *e* in Scheme 3); and (c) the intramolecular transfer of a methyl group from a methoxo group to the hemicarbonate (compare to step *d* in Scheme 2).

The intramolecular methyl transfer in the Nb-catalyst (see also Scheme 2, step *d*) has the TS with the highest energy. If such unfavourable energetics is coupled with the probability that the two reactive moieties ($-OCH_3$ and $-OC(O)OCH_3$) are within the interaction distance on the surface of the heterogeneous catalyst for the reaction to occur, one can infer that the methyl transfer between surface-bound species is less likely to occur than the methyl transfer to "surface-$OC(O)OCH_3$" from gas-phase methanol. In the latter case, two routes are open as mentioned above. The route based on the interaction of a single molecule of methanol (Scheme 3, steps *e*–*e*′) with the "surface-$OC(O)OCH_3$" moiety has a higher TS energy (Scheme 4B) than the route based on the interaction of two methanol molecules (Scheme 3, step *f*) with the hemicarbonate (Scheme 4A). The tri-molecular mechanism operating when two molecules of methanol interact with one hemicarbonate moiety may appear entropy forbidden. As a matter of fact DFT studies have clearly shown that if the hydration or alcoholysis of a substrate occurs with the formation of six (or larger) member rings the enthalpic factor is considerably lowered [27b,66], so that the reaction becomes thermodynamically more favoured. For example, the addition of methanol to CyN=C=NCy (DCC) to afford the isourea $CyH-C(OCH_3)=NCy$ has an enthalpy of 34 kcal mol^{-1} when one molecule of methanol reacts with one of the DCC, while if a trimolecular process is considered (two mol of methanol per DCC) (Scheme 5) the enthalpy is as low as 9 kcal mol^{-1}.

In order to give an experimental evidence to the mechanism based on the attack by the gas-phase methanol we have integrated DRIFT with solid state or solution multinuclear NMR studies and investigated the reaction of the hemicarbonate moiety with methanol under different reaction conditions. The sample of Al_2O_3–CeO_2 catalyst was monitored using the solid state ^{13}C NMR technique before and after exposure to methanol: a new signal due to the $-OCH_3$ group appeared at 49 ppm (Fig. 6b).

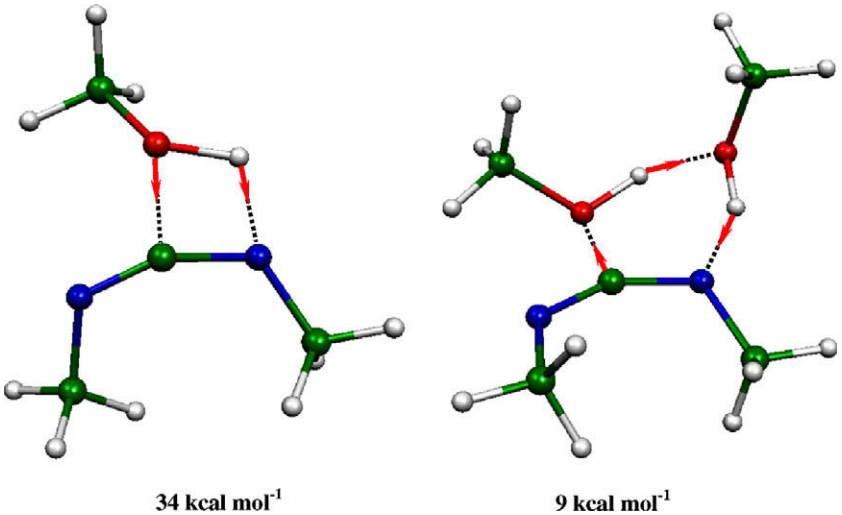

Scheme 5. Energy for the addition of methanol to DCC. The interaction of two molecules of methanol has a lower enthalpy than the direct addition of a single molecule.

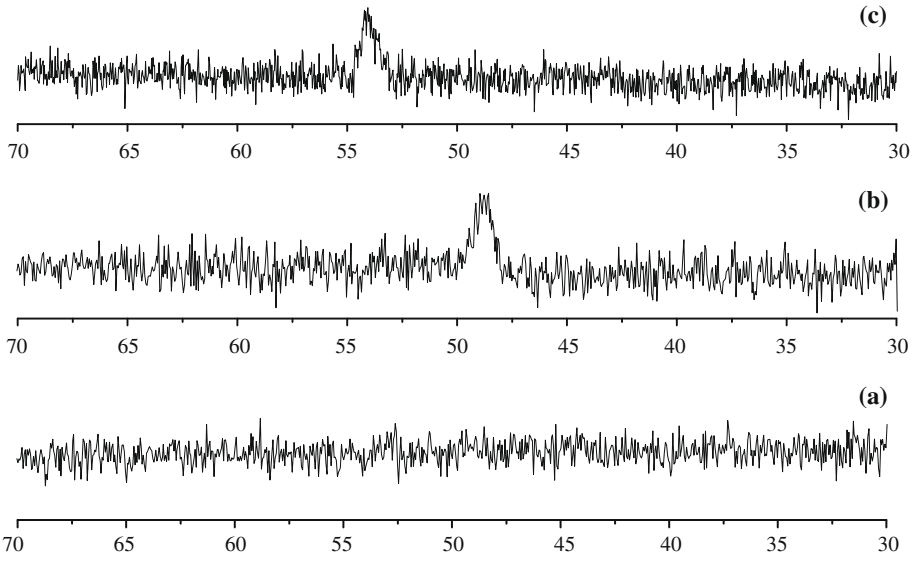

Fig. 6. ^{13}C solid state NMR of (a) Ce/Al-mixed oxide, (b) Ce/Al-mixed oxide treated with MeOH, (c) sample (b) treated with CO_2.

After reaction of such sample with CO_2, the above signal disappeared and the signal of the methyl group of the hemicarbonate –OC(O)O*C*H$_3$ very selectively appeared at 54 ppm (Fig. 6c). The signal of the O*C*(O) moiety was low in intensity and placed at 160 ppm. These assignments match very well the values found for the homogeneous species Nb(OCH$_3$)[OC(O)OCH$_3$] which shows signals at 48.7, 54.3 and 160.5 ppm, respectively, due to the methoxo, hemicarbonate-methyl and carbonate-C [27]. The sample of the catalyst was then divided into four equal parts. The first was heated in the solid state and monitored by NMR and GC–MS (gas phase) as specified in Section 2: new signals due to the formation of DMC did not appear. Similarly, when the second portion was heated in toluene, DMC was not detected.

The third portion of the carboxylated catalyst was treated with gaseous methanol at 408 K in a closed tube. The GC–MS analysis of the gas phase showed the presence of DMC (as confirmed by comparison with an authentic sample) while the solid, monitored by ^{13}C CP-MAS, showed the loss of the signals due to the hemicarbonate moiety. Similarly, when the fourth portion of the sample of the carboxylated catalyst was heated at 408 K in toluene-containing methanol, the solution clearly showed the formation of DMC in the liquid phase (^1H signal at 3.8 ppm due to the –CH$_3$ moieties and ^{13}C signals at 54.8 and 160.5 ppm due to the *C*H$_3$ and C=O moieties, respectively).

Such features clearly support the hypothesis that the formation of DMC occurs through the pathway depicted in Scheme 3 that implies the gas-phase attack of methanol on the surface-bound hemicarbonate moiety, most likely through the pathway depicted in step *f* in the above Scheme. That two molecules of methanol may be implied in the formation of DMC is demonstrated by the effect of the concentration of methanol in the gas phase when a single-phase sc-CO_2–CH_3OH mixture is reacted in the presence of CeO_2–Al_2O_3 catalyst. Fig. 7 shows that increasing the ratio of CH_3OH/CO_2 in the sc-gas phase the rate of formation of DMC sensibly increases. This is in agreement with what was found for the Nb(OCH$_3$)$_4$(OCOOCH$_3$) homogeneous catalyst [27] and the energetics of the carboxylation reaction modelled for the latter system Scheme 4.

We are now making an attempt to model the heterogeneous system (CeO_2–Al_2O_3) by DFT calculations applied to the solid surface, a task made complex by the presence of Al_2O_3 and the need of a correct modelling of its role on the surface.

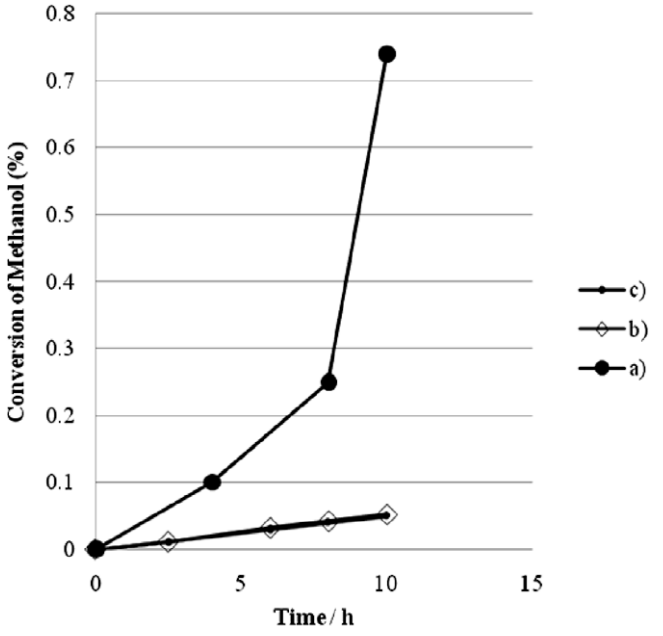

Fig. 7. Comparison of the kinetics of formation of DMC under [Nb(OMe)$_5$]$_2$ catalysis using different MeOH/CO_2 ratios at 408 K: (a) methanol and carbon dioxide (5.0 MPa) (molar ratio MeOH/CO_2 > 10); (b) methanol and sc-CO_2 (30.0 MPa) (molar ratio MeOH/CO_2 ⩽ 2); (c) methanol and sc-CO_2 (20.0 MPa) (molar ratio MeOH/CO_2 ⩽ 1).

4. Conclusions

The data reported in this paper demonstrate that the de-activation of the commercial CeO_2 catalyst is mainly due to a surface modification produced by the Ce(IV) to Ce(III) reduction under the operative conditions. Such reduction is coupled with the oxidation of methanol to other C1 molecules, among which formate has been detected by DRIFT on the surface of CeO_2. Such effect is almost completely repressed if nanoparticles of ceria loaded with 3–10% alumina are used in catalysis. Al loading causes a strong stabilisation of the catalyst that can be used for several cycles without any de-activation and reaching an apparent TON of several thousands. The dimension of the particles plays a critical role in

catalysis: nanoparticles with a 5–20 nm size seem to be the most active. Using a multi-technique approach we have investigated the reaction mechanism of DMC formation on the heterogeneous catalyst and demonstrated that it matches what we have found for homogeneous catalysts [26,32]. ^{13}C CP-MAS has been very useful in the identification of the surface-species [$-OCH_3$, $-OC(O)OCH_3$] and following their evolution in both the presence and absence of gas-phase methanol. Our studies have permitted to demonstrate that the formation of DMC takes place *via* the interaction of surface $-OC(O)OCH_3$ species with gas-phase methanol more than with the surface-bound OCH_3 species.

Acknowledgments

The financial support by the EU-IP TOPCOMBI and the Hungarian Research Foundation (OTKA, K-60549) is gratefully acknowledged. One of us (CP) gratefully acknowledges a Post-Doc grant from the University of Bari and MiUR. The authors thank Mr. Giuseppe Chita of the Institute of Crystallography, CNR, Bari, Italy, for the technical assistance during XRD registration and Mr. Giuseppe Cosmai of the Department of Chemistry of the University of Bari, Bari, Italy for the construction of the 4×-parallel autoclave.

References

[1] W.B. Kim, U.A. Joshi, J. Lee, Ind. Eng. Chem. Res. 43 (9) (2004) 1897.
[2] S. Fukuoka, M. Kawamura, K. Komiya, M. Tojo, H. Hachiya, K. Hasegawa, M. Aminaka, H. Okamoto, I. Fukawa, S. Konno, Green Chem. 5 (2003) 497.
[3] D.S. Tong, J. Yao, Y. Wang, H.-Y. Niu, G.Y. Wang, J. Mol. Catal. A: Chem. 268 (1, 2) (2007) 120.
[4] T. Chen, H. Han, J. Yao, G. Wang, Catal. Commun. 8 (9) (2007) 1361.
[5] Z. Du, W. Kang, T. Cheng, J. Yao, G. Wang, J. Mol. Catal.: Chem. 246 (1–2) (2006) 200.
[6] F. Mei, Z. Pei, G. Li, Org. Proc. Res. Dev. 8 (3) (2004) 372.
[7] S.R. Kirumakki, N. Nagaraju, K.V.R. Chary, S. Narayanan, Appl. Catal., A: Gen. 248 (1–2) (2003) 161.
[8] A.B. Shivarkar, S.P. Gupte, R.V. Chaudhari, J. Mol. Catal. A: Chem. 226 (1) (2005) 49.
[9] S.R. Kirumakki, N. Nagaraju, K.V.R. Chary, S. Narayanan, J. Catal. 221 (2) (2004) 549.
[10] N. Nagaraju, G. Kuriakose, New J. Chem. 27 (4) (2003) 765.
[11] M.B. Talawar, T.M. Jyothi, T. Raja, B.S. Rao, P.D. Sawant, Green Chem. 2 (6) (2000) 266.
[12] K. Sreekumar, T. Mathew, S.P. Mirajkar, S. Sugunan, B.S. Rao, Appl. Catal., A: Gen. 201 (1) (2000) L1.
[13] T. Beutel, J. Chem. Soc., Faraday Trans. 94 (7) (1998) 985.
[14] M. Distaso, E. Quaranta, Tetrahedron 60 (2004) 1531.
[15] G. Kuriakose, J.B. Nagy, N. Nagaraju, Catal. Commun. 6 (1) (2005) 29.
[16] R. Luque, J.M. Campelo, T.D. Conesa, D. Luna, J.M. Marinas, A.A. Romero, New J. Chem. 30 (8) (2006) 1228.
[17] G. Vasapollo, G. Mele, A. Maffei, R. Del Sole, Appl. Organomet. Chem. 17 (11) (2003) 835.
[18] X. Jiang, A. Tiwari, M. Thompson, Z. Chen, T.P. Cleary, T.B.K. Lee, Org. Proc. Res. Dev. 5 (6) (2001) 604.
[19] S.R. Kirumakki, N. Nagaraju, K.V.V.S.B.S.R. Murthy, S. Narayanan, Appl. Catal., A: Gen. 226 (1–2) (2002) 175.
[20] V. Serini, Ullmann's Enciclopedia of Industrial Chemistry, vol. A5, VCH Publishers, Weinheim, 1992, p. 197.
[21] U. Romano, R. Tesei, M.M. Massi, P. Rebora, Ind. Eng. Chem. Prod. Res. Dev. 19 (3) (1980) 396.
[22] U. Romano, Chim. Ind. Milan 75 (4) (1993) 303.
[23] K. Nishihira, S. Tanaka, K. Kodama, T. Kaneko, Eur. Pat. Appl. EP. 501, 507, 1992.
[24] D. Ballivet-Tkatchenko, S. Chambrey, R. Keiski, R. Ligabue, L. Plasseraud, P. Richard, H. Turunen, Catal. Today 115 (1–4) (2006) 80.
[25] D. Ballivet-Tkatchenko, O. Douteau, S. Stutzmann, Organometallics 19 (2000) 4563.
[26] M. Aresta, A. Dibenedetto, C. Pastore, Inorg. Chem. 42 (10) (2003) 3256.
[27] (a) M. Aresta, A. Dibenedetto, C. Pastore, Catal. Today 115 (2006) 88;
(b) M. Aresta, A. Dibenedetto, C. Pastore, I. Pápai, G. Schubert, Top. Catal. 40 (1–4) (2006) 71.
[28] T. Sakakura, J.C. Choi, H. Yasuda, Chem. Rev. 107 (2007) 2365.
[29] T. Sakakura, Y. Saito, J.C. Choi, T. Masuda, T. Sako, T. Oriyama, J. Org. Chem. 64 (1999) 4506;.
[30] T. Sakakura, Y. Saito, M. Okano, J.C. Choi, T. Sako, J. Org. Chem. 63 (1998) 7095.
[31] J.C. Choi, L.N. He, H. Yasuda, T. Sakakura, Green Chem. 4 (2002) 230.
[32] (a) M. Aresta, A. Dibenedetto, E. Fracchiolla, P. Giannoccaro, C. Pastore, I. Pápai, G. Shubert, J. Org. Chem. 70 (16) (2005) 6177;
(b) M. Aresta, A. Dibenedetto, P. Stufano, Patent application, 2009.
[33] K. Tomishige, Y. Furusawa, Y. Ikeda, M. Asadullah, K. Fujimoto, Catal. Lett. 76 (2001) 71.
[34] K. Tomishige, Y. Yoshida, Y. Arai, S. Kado, K. Kunimori, Catal. Today 115 (2006) 95.
[35] K. Tomishige, T. Sakaihori, Y. Ikeda, K. Fujimoto, Catal. Lett. 58 (1999) 225.
[36] K. Tomishige, T. Sakaihori, Y. Ikeda, K. Fujimoto, J. Catal. 192 (2000) 355.
[37] S.H. Zhong, L. L Kong, H.S. Li, X.F. Xiao, Ranliao Huaxue Xuebao 30 (5) (2002) 454.
[38] D.D. Perrin, W.L.F. Armarego, D.R. Perrin, Purification of Laboratory Chemicals, Pergamon Press, Oxford, England, 1986.
[39] Bruker AXS, DIFFRACplus EVA, EVA Application, Version 8, 0, 0, 2, Bruker AXS, Karlsruhe, Germany
[40] A. Altomare, M.C. Burla, M. Camalli, B. Carrozzini, G. Cascarano, C. Giacovazzo, A. Guagliardi, A.G.G. Moliterni, G. Polidori, R. Rizzi, J. Appl. Crystallogr. 32 (1999) 339.
[41] J. Rodríguez-Carvajal, Physica B 192 (1993) 55.
[42] Bruker AXS, TOPAS, Version 2.0, Bruker AXS, Karlsruhe, Germany.
[43] R.A. Young, The Rietveld Method, IUCR Monographs on Crystallography 5, Oxford University Press, Oxford, 1993.
[44] (a) M. Aresta, A. Dibenedetto, C. Pastore, C. Cuocci, B. Aresta, S. Cometa, E. De Giglio, Catal. Today 137 (2008) 125;
(b) M. Aresta, A. Dibenedetto, C. Pastore, C. Cuocci, B. Aresta, S. Cometa, E. De Giglio, TOPCOMBI EU Project: Technical Report, 2008.
[45] R. Sasikala, V. Sudarsan, S.K. Kulshreshtha, J. Solid State Chem. 169 (2002) 113.
[46] A.D.J. Becke, Chem. Phys. 98 (1993) 5648.
[47] C. Lee, W. Yang, R.G. Parras, Phys. Rev. B 37 (1988) 785.
[48] P.J. Stephens, F.J. Devlin, C.F. Chabalowski, M.J. J Frisch, J. Phys. Chem. 98 (1994) 11623.
[49] M. Dolg, H. Stoll, H. Preuss, R.M. Pitzer, J. Phys. Chem. 97 (1993) 5852.
[50] T.H. Dunning Jr., J. Chem. Phys. 52 (1970) 2823.
[51] T.H. Dunning Jr., P.J. Hay, in: H.F. Schaefer III (Ed.), Methods of Electronic Structure Theory, Plenum Press, 1977.
[52] H.F. Schaefer III, J. Chem. Phys. 83 (1985) 5721.
[53] M.J. Frisch, G.W. Trucks, H.B. Schlegel, G.E. Scuseria, M.A. Robb, J.R. Cheeseman, J.A. Montgomery Jr., T. Vreven, K.N. Kudin, J.C. Burant, J.M. Millam, S.S. Lyengar, J. Tomasi, V. Barone, B. Mennucci, M. Cossi, G. Scalmani, N. Rega, G.A. Petersson, H. Nakatsuji, M. Hada, M. Ehara, K. Toyota, R. Fukuda, J. Hasegawa, M. Ishida, T. Nakajima, Y. Honda, O. Kitao, H. Nakai, M. Klene, X. Li, J.E. Knox, H.P. Hratchian, J.B. Cross, C. Adamo, J. Jaramillo, R. Gomperts, R.E. Stratmann, O. Yazyev, A.J. Austin, R. Camml, C. Pomelli, J.W. Ochterski, P.Y. Ayala, K. Morokuma, G.A. Voth, P. Salvador, J.J. Dannenberg, V.G. Zakrzewski, S. Dapprich, A.D. Daniels, M.C. Strain, O. Farkas, D.K. Malick, A.D. Rabuck, K. Raghavachari, J.B. Foresman, J.V. Ortiz, Q. Cui, A.G. Baboul, S. Clifford, J. Cioslowski, B.B. Stefanov, G. Liu, A. Liashenko, P. Piskorz, I. Komaromi, R.L. Martin, D.J. Fox, T. Keith, M.A. Al-Laham, C.Y. Peng, A. Nanayakkara, M. Challacombe, P.M.W. Gill, B. Johnson, W. Chen, M.W. Wong, C. Gonzalez, J.A. Pople, Gaussian 03, Revision C.02, Gaussian, Inc., Pittsburgh, PA, 2004.
[54] J.Z. Shyu, W.E. Weber, H.S. Gandhi, J. Phys. Chem. 92 (17) (1988) 4964.
[55] E. Finocchio, M. Daturi, C. Binet, J.C. Lavalley, G. Blanchard, Catal. Today 52 (1999) 53.
[56] M. Daturi, C. Binet, J.C. Lavalley, A. Galtayries, R. Sporken, Phys. Chem. Chem. Phys. 1 (1999) 5717.
[57] M.M. Natile, G. Boccaletti, A. Glisenti, Chem. Mater. 17 (2005) 6272.
[58] F.P. Rotzinger, J.M. Kesselman-Truttmann, S.J. Hug, V. Shklover, M. Gratzel, J. Phys. Chem. B 108 (2004) 5004.
[59] K. Taek Jung, A.T. Bell, J. Catal. 204 (2001) 339.
[60] D.J. Darensbourg, M.W. Holtcamp, Coord. Chem. Rev. 153 (1996) 155.
[61] L. Pauling, The Nature of the Chemical Bond, third ed., Cornel University Press, Ithaca, NY, 1960.
[62] D. Terribile, A. Trovarelli, C. de Leitenburg, A. Primavera, G. Dolcetti, Catal. Today 47 (1999) 133.
[63] R.D. Shannon, Acta Crystallogr. A 32 (1976) 751.
[64] K.T.J. Alexis, T. Bell, Top. Catal. 20 (2002) 97.
[65] M. Aresta, A. Dibenedetto, P. Giannoccaro, C. Pastore, I. Papai, G. Schubert, Eur. J. Inorg. Chem. 5 (2006) 908.
[66] F. Tordini, A. Bencini, M. Bruschi, L. De Gioia, G. Zampilla, P. Fantucci, J. Phys. Chem. A 107 (8) (2003) 1188.